Supporting Information for Drivers and reversibility of abrupt ocean state transitions in the Amundsen Sea, Antarctica

Justine Caillet[1], Nicolas C. Jourdain[1], Pierre Mathiot[1], Hartmut H. Hellmer[2], Jérémie Mouginot[1]

[1]Univ. Grenoble Alpes, CNRS, IRD, Grenoble INP, IGE, 38000 Grenoble, France

[2]Alfred Wegener Institute Helmholtz Centre for Polar and Marine Research, Bremerhaven, Germany

Contents of this file

Introduction This supplementary document describes the calibration and evaluation of the reference simulation. It includes a description of both the observational data sets used to validate the configuration (see Section S1) and sensitivity experiments carried out in this study (see Section S2 and Table S1). The evaluation of these sensitivity experiments are made through the analysis of sea-ice extent (see Section S3 and Figure S1), temperature profiles (see Section S4 and Figure 2) and basal melt rates (see Section S5 and Figure S3).

S1. Observational Data Sets

The model is evaluated over the period 2012-2018 through a comparison with available observational datasets relative to sea-ice concentration, temperature profiles, and ice-shelves melt rates.

We used 1607 Conductivity-Temperature-Depth (CTD) profiles collected during summer campaigns from 1994 to 2018 (Dutrieux et al., 2014; Heywood et al., 2016) to evaluate the simulated temperature field. Individual CTD profiles are interpolated vertically onto the 75 vertical levels of our model configuration. The comparison to CTD data is performed by sampling model outputs in space (nearest profile) and time (linear interpolation between monthly outputs) following the actual CTD station distribution.

To evaluate the simulated sea-ice cover, the model outputs are compared to the NOAA/NSIDC Climate Data Record (CDR) of the Passive Microwave Sea-Ice Concentration dataset, version 4 (Meier et al., 2022), which provides daily and monthly estimates of sea-ice concentration in the polar regions for the period 1987-2020 on a 25 $\times$ 25 km stereographic grid. The observational data are interpolated onto the model grid and only concentration values above 0.15 are considered in both the model and observations due to observational uncertainties for lowest concentrations.

Finally, the simulated ice-shelf basal melt rates over the period 2012-2018 are compared to estimates based on satellite observations (Adusumilli et al., 2020).

S2. Sensitivity experiments

Preliminary to our main study, several sensitivity experiments were carried out in order to improve the fidelity of the model, in particular its ability to correctly represent ice-shelf basal melting. Their main characteristics are detailed in Tab. S1. In view of the shortcomings of the initial simulation (INITIAL), we explored three distinct ways

to improve the representativeness of the model: (i) vertical mixing parameterization, (ii) forcing, and (iii) parameterization of melting under ice shelves.

The diffusivity and vertical turbulent viscosity coefficients are derived from a turbulent closure model that does not allow the thermocline depth to be represented correctly, particularly in the Southern Ocean (Rodgers et al., 2014). The thermocline depth is often too high in summer and when it is windy, as observed in INITIAL. To compensate for the lack of representation of some processes, an ad hoc parameterization exists in NEMO (see "TKE scheme" in Madec & the NEMO Team, 2016) to inject an amount D of additional turbulent kinetic energy below the mixed layer, with D defined as:

$$D = (1 - f_i)\, f_r e_s e^{-\frac{z}{h_\tau}} \tag{1}$$

where f_i is the sea-ice concentration, f_r the fraction of surface turbulent kinetic energy penetrating below the mixed layer, e_s the surface boundary condition of the turbulent kinetic energy (diagnosed by the TKE scheme), z the depth, and h_τ the vertical mixing length scale. To lower the depth of the thermocline, we modify the f_r parameter in EFR by taking the maximum value suggested by Madec (2008); Heuzé et al. (2015). In HTAU, we modify the vertical mixing length to $h_\tau = 60\,\mathrm{m}$, which is appropriate for high latitudes (Rodgers et al., 2014).

One of the main sources of divergence between our simulations and the observations is due to uncertainties in the forcing. We tested the model sensitivity to oceanic and atmospheric forcing. The BDY experiment includes the correction of oceanic lateral boundaries to match the World Ocean Atlas 2018 seasonal climatology (Garcia et al., 2019), and BDY + HTAU + FORCING takes into account another atmospheric reanalysis product, DFS5.2

(Dussin et al., 2016). The BDY + HTAU is a combination of the changes made both in BDY and HTAU.

Finally, in order to improve the basal melt rates, especially under Getz, Thwaites and Pine Island ice shelves, several corrections are explored. BDY + HTAU + GAMMA corrects basal melt rates through a modification of the heat and salt exchange coefficients (Γ_T and Γ_S, respectively). According to Jourdain et al. (2017), melt rates are proportional to $\Gamma^{1.25}$ where Γ is the heat/salinity exchange coefficient. Since melting under Getz was too high by about 1/3, the coefficients were multiplied by $\frac{2}{3}^{\frac{1}{1.25}}$ to reduce the melt rate by one third. The partial collapse of Thwaites Ice Shelf in 2015 altered the topography significantly. To assess the influence of topography on the melt rates under Thwaites Ice Shelf, the Rtopo2 topography (Schaffer et al., 2016) prior to the collapse of the ice shelf is used in BDY + HTAU + GAMMA + TOPO.

S3. Evaluation of sensitivity experiments: Sea-ice extent

The sea-ice cover analysis gives an insight into the seasonal variability (CTD profiles are collected only in austral summer and basal melt rates are often estimated over several years). In all our simulations, the seasonal variability is well represented (see Fig. S1) although the simulated summer and winter extrema differ from those in the NOAA/NSIDC climatology. Sea-ice extent is very sensitive to lateral boundary conditions. The correction of lateral boundaries to the World Ocean Atlas 2018 (BDY) results in an overestimation of the sea-ice extent (+35% in autral summer and +17% in winter), which hides an overestimation in the deep ocean and an underestimation in front of the ice shelves. The sea-ice extent is also sensitive to the stratification of the water column (HTAU). The change in vertical mixing leads to an underestimated sea-ice extent (-2% in austral summer -16%

in winter). The choice of atmospheric forcing impacts mostly the summer sea-ice cover, while changes in the vertical mixing parameter f_r, topography, and heat and salt exchange coefficients do not affect the sea-ice extent.

S4. Evaluation of sensitivity experiments: Temperature profiles

The CTD profiles measured in front of the Pine Island–Thwaites and Dotson–Getz ice shelves suggest a different flow pattern between the western and eastern continental shelf, consistent with Wåhlin et al. (2012); Dotto et al. (2019). The waters are generally 0.5°C warmer in the Pine Island–Thwaites area where CDW onshore flow is facilitated.

In front of the Pine Island–Thwaites ice shelves, INITIAL overestimates the subsurface temperature (0-400 m) by 1°C and the bottom temperature (800-1200 m) by 0.5°C, and the thermocline is too shallow by 200 m (Fig. S2). The ocean boundary correction with the World Ocean Atlas 2018 results in a significant change in the water column of the deep ocean. As the near-bottom temperature is essentially determined by the oceanic conditions at the shelf break, this correction lowers the temperature by about 0.5°C and thus approaches the observations in the lower part of the water column (deviation from observations less than 0.2°C below 600 m), although the thermocline is still too shallow. The increased vertical mixing length scale lowers the overestimated thermocline depth. Above 500 m, the temperature is lowered by an average of 0.5°C, but it is still higher than the CTD profiles (0.5°C on average). The other sensitivity tests have little impact on the temperature of the water column (0.2°C down to 300 m).

Concerning Dotson–Getz ice shelves, INITIAL overestimates the bottom temperature (800-1200 m) by 0.5°C, and the thermocline is again too shallow by 200 m (Fig. S2). The ocean boundary correction with the World Ocean Atlas 2018 lowers the temperature by

about 0.5°C, resulting in a deviation from observations of less than 0.2°C. The increased vertical mixing length scale lowers the overestimated thermocline depth by 100 m, but has also an impact on near bottom temperature as does the change in the values of the heat and salt exchange coefficients.

S5. Evaluation of sensitivity experiments: Basal melt rates

We evaluate our basal melt rates by comparing them to satellite data estimates from Adusumilli et al. (2020) despite large uncertainties. Simulated cavity melt rates are close to published estimates for Venable, Abbot, and Cosgrove, underestimated for Pine Island and Thwaites (-30% and -77%, respectively for BDY + HTAU), although the vertical temperature distribution is overestimated by 0.5°C in front of these ice shelves, and overestimated for Crosson, Dotson and Getz (337%, 98% and 119%, respectively for BDY + HTAU) (see Fig. S3). In general, the interannual variation in melting is not as large as observed. Due to proportionality, a unique modification of the melt rates (BDY + HTAU + GAMMA) does not improve the overall results. Thus, we prefer to keep the original heat and salt exchange coefficients (Γ_T and Γ_S) in order to simulate correct melt rates for Pine Island rather than Getz ice shelf, which was already problematic when setting up Nemo's cavity module (Mathiot et al., 2017). The gain from the change in ice topography at Thwaites (BDY + HTAU + GAMMA + TOPO) is negligible.

S6. Conclusion on the sensitivity experiments

We selected the simulation (BDY + HTAU) as the reference simulation from which simulations with perturbations were built. The reference simulation captures well the seasonal variability with an average sea-ice extent error in austral summer and winter, of, respectively, 31% and 6%. The temperature between 700 and 1200 m depth is well

represented on the shelf (deviation from observations less than 0.2°C). The thermocline is still too shallow, which corresponds to an overestimation of the temperature between 300 m and 600 m depth of about 0.5°C. Simulated basal melt rates are close to published estimates for Venable, Abbot and Cosgrove, underestimated for Pine Island and Thwaites (-30% and -77%, respectively), and overestimated for Crosson, Dotson and Getz (337%, 98% and 119%, respectively).

References

Adusumilli, S., Fricker, H. A., Medley, B., Padman, L., & Siegfried, M. R. (2020). Interannual variations in meltwater input to the Southern Ocean from Antarctic ice shelves. *Nature Geoscience*, *13*(9). doi: 10.1038/s41561-020-0616-z

Dotto, T. S., Garabato, A. C., Bacon, S., Holland, P. R., Kimura, S., Firing, Y. L., ... Jenkins, A. (2019). Wind-driven processes controlling oceanic heat delivery to the amundsen sea, antarctica. *Journal of Physical Oceanography*, *49*(11). doi: 10.1175/JPO-D-19-0064.1

Dussin, R., Barnier, B., Brodeau, L., & Molines, J. M. (2016). The making of the drakkar forcing set dfs5. *DRAKKAR/MyOcean Rep*, *104*, 16.

Dutrieux, P., De Rydt, J., Jenkins, A., Holland, P. R., Ha, H. K., Lee, S. H., ... Schröder, M. (2014). Strong sensitivity of pine Island ice-shelf melting to climatic variability. *Science*, *343*(6167). doi: 10.1126/science.1244341

Garcia, H., Boyer, T., Baranova, O., Locarnini, R., Mishonov, A., Grodsky, A., ... Zweng, M. (2019). World Ocean Atlas 2018: Product Documentation.

Heuzé, C., Ridley, J. K., Calvert, D., Stevens, D. P., & Heywood, K. J. (2015). Increasing vertical mixing to reduce Southern Ocean deep convection in NEMO3.4. *Geoscientific*

Model Development, *8*(10). doi: 10.5194/gmd-8-3119-2015

Heywood, K. J., Biddle, L. C., Boehme, L., Dutrieux, P., Fedak, M., Jenkins, A., ... others (2016). Between the devil and the deep blue sea: The role of the Amundsen Sea continental shelf in exchanges between ocean and ice shelves. *Oceanography*, *29*(4), 118–129.

Jourdain, N. C., Mathiot, P., Merino, N., Durand, G., Le Sommer, J., Spence, P., ... Madec, G. (2017). Ocean circulation and sea-ice thinning induced by melting ice shelves in the Amundsen Sea. *Journal of Geophysical Research: Oceans*, *122*(3). doi: 10.1002/2016JC012509

Madec, G. (2008). Nemo ocean general circulation model reference manuel. *Paris: LODYC/IPSL*.

Madec, G., & the NEMO Team. (2016). NEMO ocean engine. *Note du Pôle de modélisation*(27).

Mathiot, P., Jenkins, A., Harris, C., & Madec, G. (2017). Explicit representation and parametrised impacts of under ice shelf seas in the z*- coordinate ocean model NEMO 3.6. *Geoscientific Model Development*, *10*(7). doi: 10.5194/gmd-10-2849-2017

Meier, W. N., Stewart, J. S., Windnagel, A., & Fetterer, F. M. (2022). Comparison of hemispheric and regional sea ice extent and area trends from noaa and nasa passive microwave-derived climate records. *Remote Sensing*, *14*(3), 619.

Rodgers, K. B., Aumont, O., Mikaloff Fletcher, S. E., Plancherel, Y., Bopp, L., De Boyer Montégut, C., ... Wanninkhof, R. (2014). Strong sensitivity of Southern Ocean carbon uptake and nutrient cycling to wind stirring. *Biogeosciences*, *11*(15). doi: 10.5194/bg-11-4077-2014

Schaffer, J., Timmermann, R., Erik Arndt, J., Savstrup Kristensen, S., Mayer, C., Morlighem, M., & Steinhage, D. (2016). A global, high-resolution data set of ice sheet topography, cavity geometry, and ocean bathymetry. *Earth System Science Data*, *8*(2). doi: 10.5194/essd-8-543-2016

Wåhlin, A. K., Muench, R. D., Arneborg, L., Björk, G., Ha, H. K., Lee, S. H., & Alsén, H. (2012). Some implications of ekman layer dynamics for cross-shelf exchange in the Amundsen sea. *Journal of Physical Oceanography*, *42*(9). doi: 10.1175/JPO-D-11-041.1

Table S1. Characteristics of sensitivity experiments used for model calibration (different terms are defined in section 1)

Simulation Name	f_r	h_τ	Boundaries	Γ_T	Γ_S	Topo	Forcing
INITIAL	0.05	$h_\tau(\phi)$	-	$2.21\,10^{-2}$	$6.19\,10^{-4}$	BedMachine	JRA55
EFR	0.10	$h_\tau(\phi)$	-	$2.21\,10^{-2}$	$6.19\,10^{-4}$	BedMachine	JRA55
BDY	0.05	$h_\tau(\phi)$	WOA18 Correction	$2.21\,10^{-2}$	$6.19\,10^{-4}$	BedMachine	JRA55
HTAU	0.05	$60\,m$	-	$2.21\,10^{-2}$	$6.19\,10^{-4}$	BedMachine	JRA55
BDY + HTAU	0.05	$60\,m$	WOA18 Correction	$2.21\,10^{-2}$	$6.19\,10^{-4}$	BedMachine	JRA55
BDY + HTAU + GAMMA	0.05	$60\,m$	WOA18 Correction	$1.60\,10^{-2}$	$4.48\,10^{-4}$	BedMachine	JRA55
BDY + HTAU + GAMMA + TOPO	0.05	$60\,m$	WOA18 Correction	$1.60\,10^{-2}$	$4.48\,10^{-4}$	RTopo2	JRA55
BDY + HTAU + FORCING	0.05	$60\,m$	WOA18 Correction	$2.21\,10^{-2}$	$6.19\,10^{-4}$	BedMachine	DFS5.2

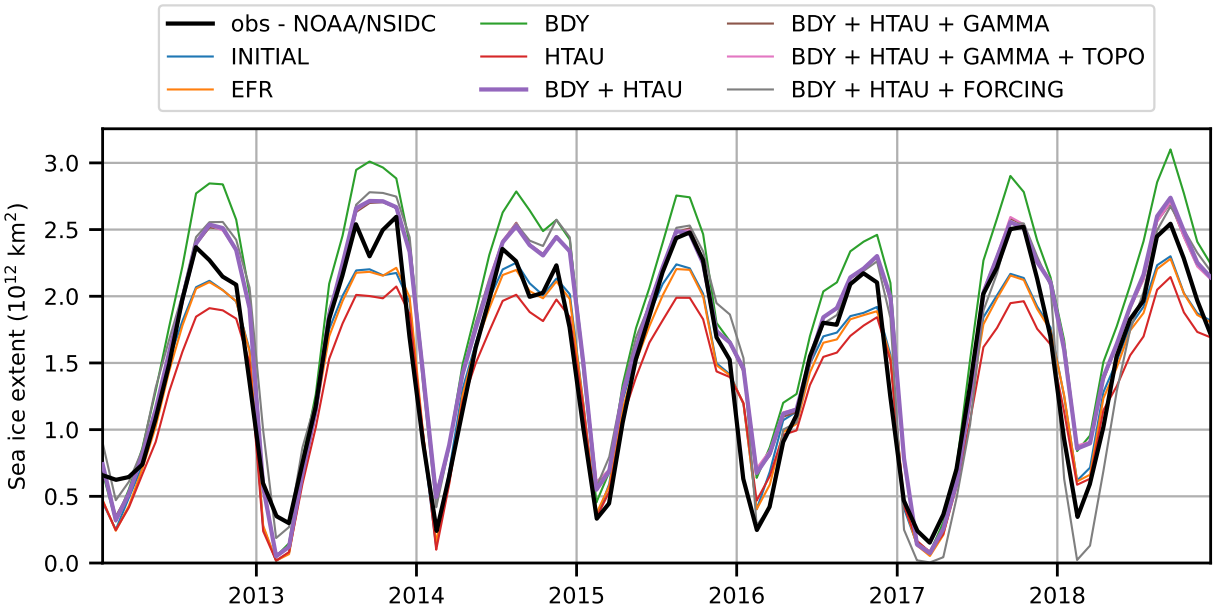

Figure S1. Variability of the sea-ice extent over the period 2012-2018 depending on the sensitivity experiments. As a reminder, only areas of sea-ice concentration greater than 0.15 were considered for the sea-ice extent estimation. The observations correspond to the NOAA/NSIDC Climate Data Record of Passive Microwave Sea-Ice Concentration dataset.

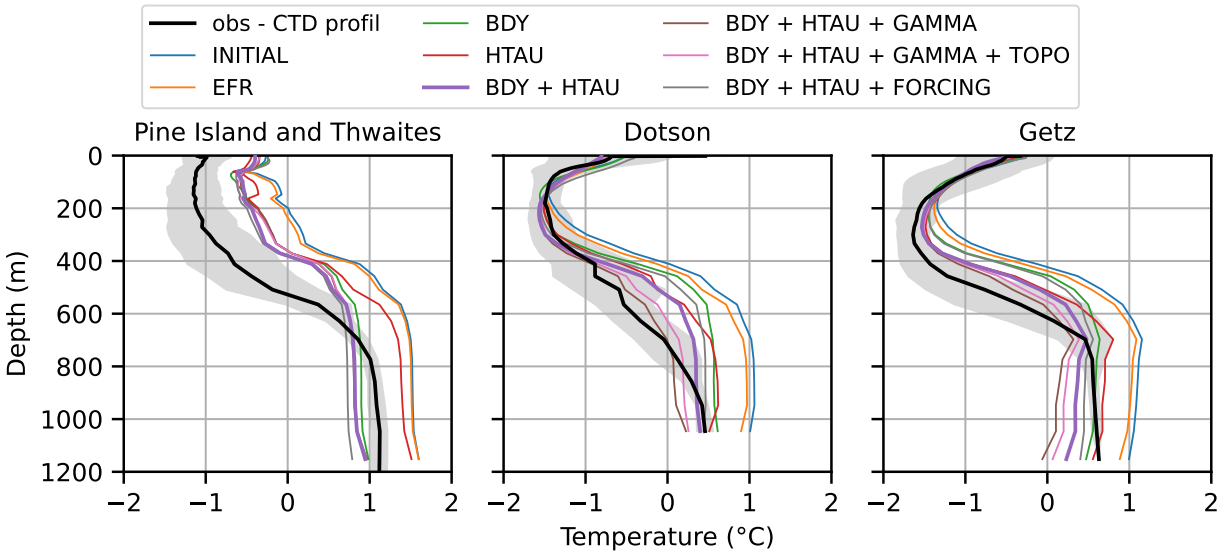

Figure S2. Mean conservative temperature profiles in front of Pine Island and Thwaites (left), Dotson(middle), and Getz (right) ice shelves depending on the sensitivity experiments. The observations are CTD profiles collected during austral summer campaigns from 2012-2018.

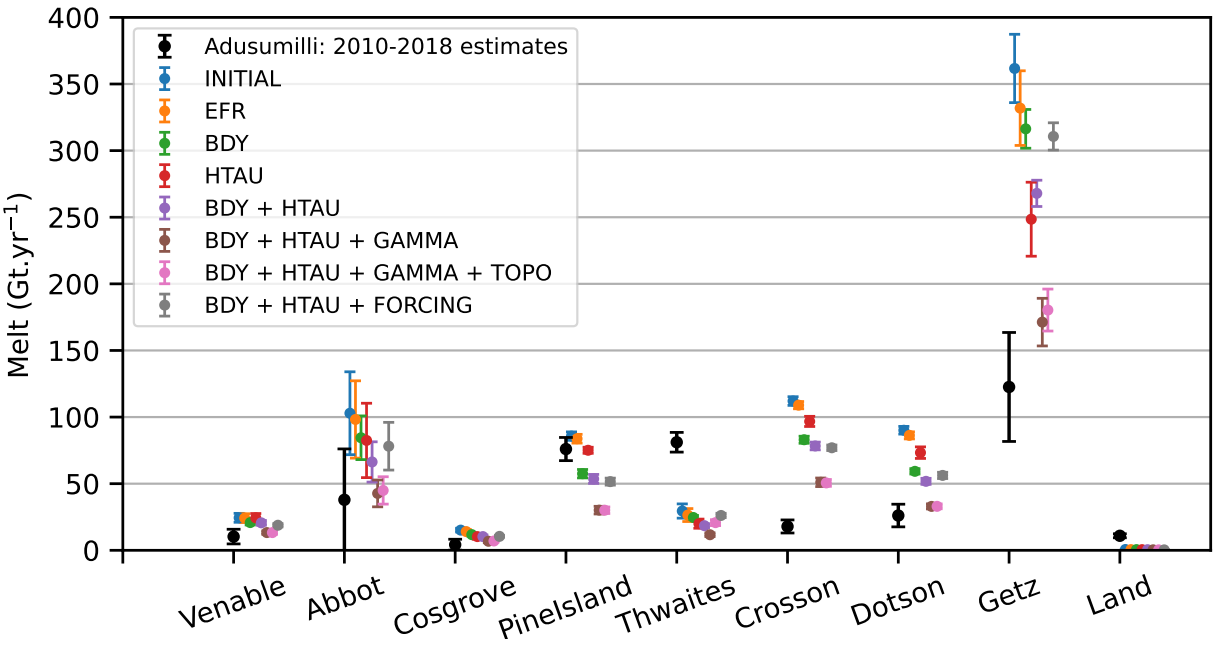

Figure S3. 2012-2018 mean basal mass loss under various Amundsen Sea ice shelves depending on the sensitivity experiments. Simulated basal mass losses are compared to the 2010-2018 estimates from Adusumilli et al. (2020)